

Factoring Surface Area for Mechanochemical Effects During Micro-scratching

Lionel Yan Jin Lee, Jianyu Tu, and Hao Wang#

Department of Mechanical Engineering, College of Design and Engineering, National University of Singapore, 9 Engineering Drive 1, 117575, Singapore
Corresponding Author / Email: mpewhao@nus.edu.sg, TEL: +65-6516-2207

KEYWORDS: Micro-scratching, Aluminum alloy, Mechanochemical effect, Chemisorption, Micro-cutting

The mechanochemical effect is beneficial to the micro-cutting process but the working mechanism and the condition for its manifestation is far from understood. This work focuses on the surface area for chemisorption to occur under the application of a surface-active medium (SAM). 0.1 μm deep nano-grooves were produced to increase the surface area of rapidly solidified aluminum (RSA6061). After which, a SAM was applied, and constant load micro-scratching tests were performed perpendicular to the nano-grooves. The manifestation of the mechanochemical effect was identified by the difference in penetration depth, which was reduced by up to 63.2% corresponding to a 18.2% increase in scratch hardness. The magnitude of the mechanochemical effect was determined by analyzing the residual depth where a progressive increase was observed with the increase in surface area over a range of 16.4–39.9%. Changes in the elastic recovery were also observed with a lower degree of recovery under chemisorption. However, the rate of increase in mechanochemical effect manifestation was not linearly dependent on the surface area, which suggests that additional geometrical factors such as the shape of the nano-grooves may also be important for consideration in understanding the conditions to support the mechanochemical effect during micro-cutting.

NOMENCLATURE

H_s	= scratch hardness
C	= scratch hardness constant
F_N	= scratch load
w	= groove width
d	= groove depth
r	= indenter radius
s	= spring back
K_I	= spring back scaling constant
H	= hardness
E	= elastic modulus
$H_{S,R}$	= scratch hardness under mechanochemical effect
$H_{S,C}$	= scratch hardness under normal conditions
s_R	= spring back under mechanochemical effect
s_C	= spring back under normal conditions
ΔH	= difference in scratch hardness
Δs	= difference in spring back

1. Introduction

Mechanochemical effects have been well established to cause

significant impacts on the machining process both on the meso- [1,2], and microscopic length scales [3,4]. This unique phenomenon involves the application of a surface-active medium (SAM) on metal surfaces to drastically degrade its mechanical stability in the form of reducing strengths [5] or causing embrittlement [6]. Multiple direct industrial benefits have been derived from this effect such as lower cutting energy, enhanced surface finish, and suppression of diamond tool wear. Recent findings even revealed the substantial influence of the mechanochemical effect on microstructural evolution on the machined surfaces where dynamic recrystallization and grain growth could occur producing large grains as compared to the typically wide distribution of smaller and highly distorted grains.

At present, the notion for this phenomenon to occur is through the change in surface energy of the work material due to bonding conditions between the SAM and work material atoms that are more favorable for new surface generation [7]. This is, therefore, classified as a surface effect in micro-cutting where the region of interest is, as implied by the definition, on the surface of the work material. Yet interestingly the surface conditions of the work material are rarely discussed. There are, however, other several notable pre-requisites for work materials to invoke this mechanochemical effect such as high ductility, low cutting speeds, and large cutting volumes [7]. Therefore, this work aims to investigate the mechanochemical effect from a new perspective of assessing the influence as a function of the surface area

given for chemisorption to occur.

2. Experimental methodology

2.1 Sample preparation

Rapidly solidified aluminum (RSA6061) was the material selected for these experiments having been established to be affected by the mechanochemical effect [8]. The sample surface was diamond turned on an ultra-precision machine (Toshiba ULG-100, Fig. 1(a)) with a spindle speed, feed rate, and nominal cutting depth of 600 rpm, 1.5 mm/min, and 4 μm . A roughness of 6 nm Sa was achieved on the flattened surface as measured on a 3D laser confocal microscope (Olympus OLS5000) without filtering (Fig. 1(b)).

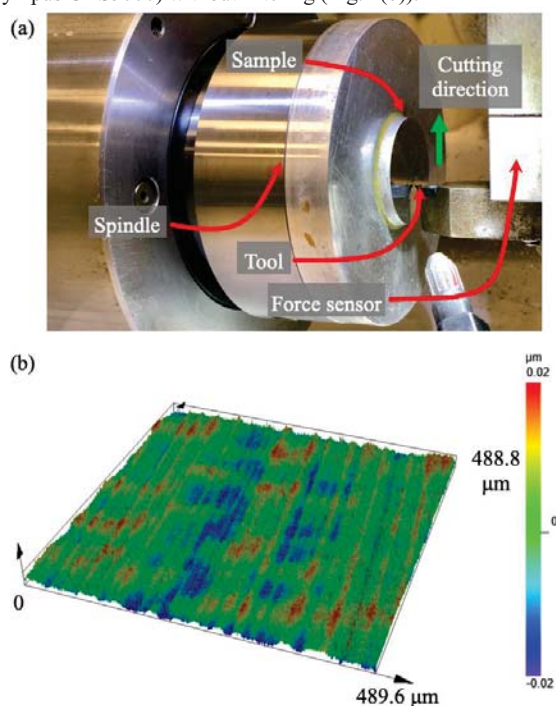


Fig. 1 Surface preparation: (a) experimental setup on an ultra-precision machine tool center; (b) 3D laser scanned image of the diamond turned surface

Subsequently, the effective surface area of the sample was modified by scribing the surface with a series of nano-grooves in the effort of creating additional area for chemisorption. These nano-grooves were fabricated using a scratch tester (Anton Paar Micro-combi³) where a constant load and speed of 0.05 N and 10 mm/min was applied through a diamond indenter (100 μm radius) that was dragged across the work material to produce these nano-grooves. Three different surface conditions were obtained by controlling the pitch between each nano-groove (36, 18, and 9 μm) to produce groove surfaces as shown in Fig. 2. These surfaces will be labelled according to their pitch as 36p, 18p and 9p, with each groove at a depth of 0.1 μm . The corresponding surface areas were measured

to be 47,593.4 μm^2 , 47,704.0 μm^2 , and 47,780.4 μm^2 for the 36p, 18p, and 9p surfaces within a measuring window of 218 \times 218 μm .

2.2 Micro-scratch tests

The sample was then rotated 90 degrees on the scratch tester (Fig. 3(a)) such that the scratch direction would be perpendicular to the nano-grooves. A surface-active medium (SAM), Dykem permanent marker ink (High purity 44), was then applied on a selected region on these nano-grooves such that a scratch would occur on a clean surface, followed by a chemisorbed surface, and back into a clean surface (Fig. 3(b)). Three scratches were performed for each surface condition at a constant load of 1 N and speed of 10 mm/min. The magnitude of the mechanochemical effect will then be compared between the different surface areas by evaluating the scratch penetration depth and residual depth obtained by probe scanning on the scratch tester and laser scanning confocal microscopic. The sample surfaces were cleaned free of SAM using ethanol prior to optical analysis.

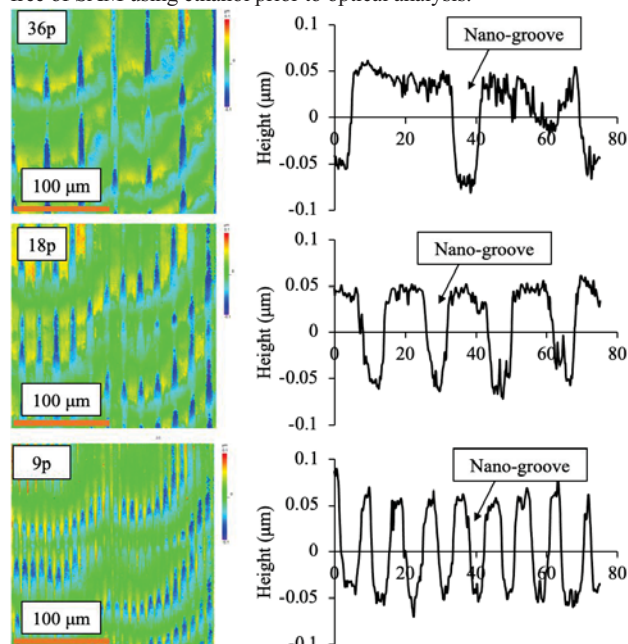


Fig. 2 Top view image of the nano-groove and the corresponding height profiles for different nano-groove pitches of 36, 18, and 9 μm

It is important to clarify that these micro-scratch tests were performed while the SAM remained purely in its liquid form. To affirm this assumption, micro-hardness measurements were performed on an as-coated RSA6061 sample with a 0.1 N load at intervals of 3 minutes. Fig. 4 presents the approximated hardness of the ink as it solidifies over time after application on the sample, which shows that the scratch tests were performed while the surfactant was still in its aqueous form, thus sufficiently neglecting implications of solid coating effects.

3. Results and discussion

3.1 Mechanochemical effect

Fig. 5 presents the profile of the penetration depth as the diamond indenter scratched the aluminum alloy surface under a constant load of 1 N. As the indenter progresses from the flat diamond-turned surface into the nano-grooved region without SAM, the material exhibits substantial plasticity with a 11.4 μm deep penetration into the sample. This occurred as a reaction to the pre-processed defect formations that were likely to degrade the mechanical stability of the surface. However, the penetration depth decreases to 4.2 μm as the indenter moves into the SAM-affected region signifying the decline in plasticity of the material. The 63.2% reduction in penetration depth corresponds to an increase in scratch hardness by 18.2% under the influence of the mechanochemical effect as determined by Eq. 1.

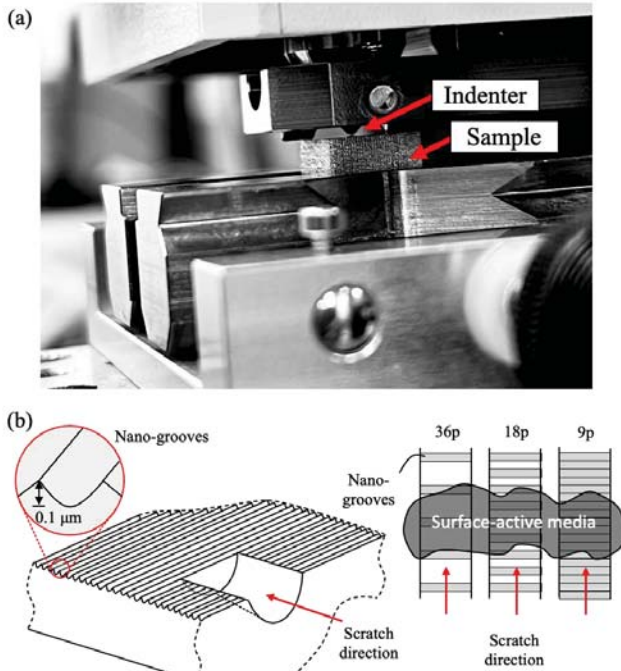


Fig. 3 Scratch test experimentation: (a) experimental setup; (b) schematic of the scratch test procedure

$$H_s = \frac{CF_N}{w^2} \quad (1)$$

$$w = 2\sqrt{2d(r-d)} \quad (2)$$

where C is a constant $8/\pi$ for a spherical indenter, F_N is the applied load, and w is the width of the groove calculated by the depth of the groove d and the radius of the indenter r . Although the mechanochemical effect has been often associated with lower cutting energies, the increase in hardness of the SAM-affected material is still consistent with the current consensus on the phenomenological impact on the material.

The mechanochemical effect on the microscopic scale was explained as the interatomic bonding between surfactant molecules and the work material atoms, such that an instability in the surface

bonds is created to promote surface generation by the breakage of workpiece atoms [7]. The surface bonds were also thought to restrict dislocation egression through the surface [8], which concentrates the stress at these pinning points to further promote surface generation. In scratch testing, chip formation is negligible due to the deformation mechanism being largely associated with ploughing and rubbing in light of the relative tool sharpness [9]. Therefore, the input energy during scratch testing would then be largely dissipated as plastic energy where the atomistic focus will be placed on dislocation mobility. High dislocation mobility enables high plastic deformation but the restriction of dislocation egression through the surface under the mechanochemical effect would correspondingly result in the observed reduced plastic deformation.

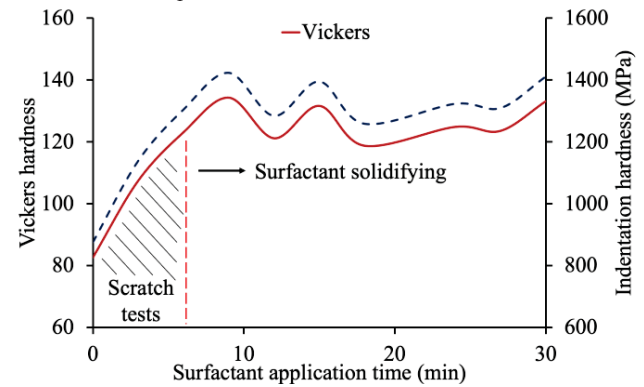


Fig. 4 Hardness measurements of the surfactant as solidification progresses over time

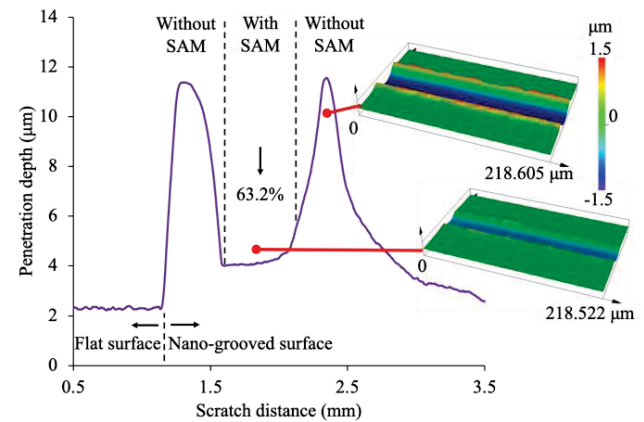


Fig. 5 Measured penetration depth (P_d) during scratching with applied load, residual depth (R_d) after the scratch, and corresponding 3D profiles of the produced scratches for regions with and without SAM under 18p surface conditions

3.2 Impact of surface area

The groove then undergoes elastic recovery where the residual groove depth further decreases to less than 1.5 μm as shown by the 3D laser scanned profiles (Fig. 5), while Fig. 6 presents the individually measured cross-sectional profiles of the scratched grooves for the different surface area conditions after recovery. In these cross-sections, the influence of the mechanochemical effect on the deformation parallel and lateral to the scratch direction were

assessed by the differences in residual depth and material side flow.

3.2.1 Residual depth

Just as the penetration depth was larger without SAM, the residual depth was also larger. Despite the minute increase in surface area with the presence of more nano-grooves on the surface, the higher area for chemisorption increased the influence of the mechanochemical effect on the material where a larger difference between the final depths of the grooves produced with and without SAM increases with surface area.

Assuming the differences in residual depths provide direct correspondence with the influence of the mechanochemical effect, the relationship between the surface area and the surface effect are evidently non-linear. This suggests a complex sequence of events that occurred under the mechanochemical effect, such that the mechanochemical effect involves more than just the area factor alone.

At this juncture, it is suspected that the geometry of the nano-grooves would also influence the impact of the mechanochemical effect. The geometry of the nano-grooves may provide the stress conditions that promote the working mechanism of the mechanochemical effect. Presently, the nano-grooves are theoretically rounded at the valley of each groove. However, when put into the perspective of the penetration depth during the scratch, these grooves may be considered V-shaped notches that is very well known to serve as a localized region for high stress concentration. The increase in such formations for localized stress concentration points couples with the mechanochemical effect to drastically change the stress state of the material during deformation. The increase in stress consequently involves the complexities of work hardening, strain softening, and thermal softening during metal working, which is unclear at this point of the investigation.

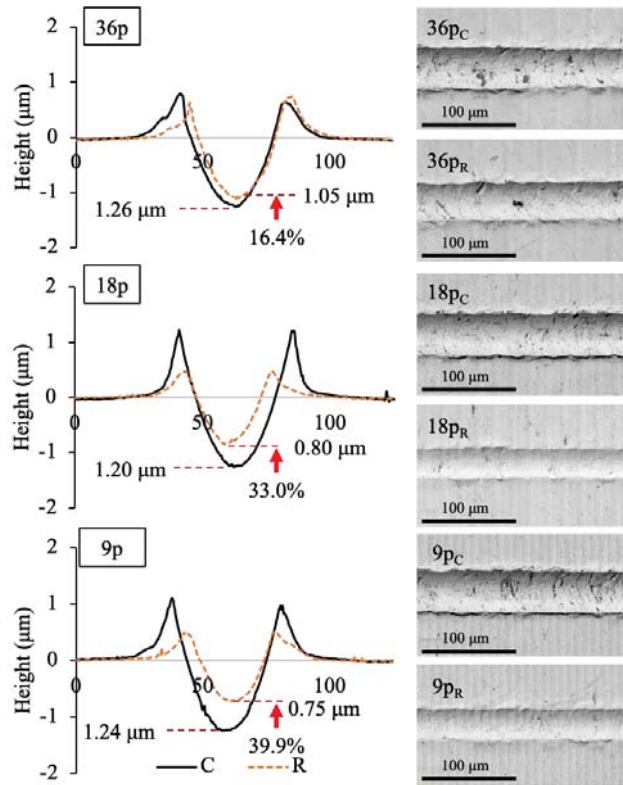


Fig. 6 Cross-sectional profile and the corresponding top view optical image of the scratches produced on different surface areas and chemisorption conditions

3.2.2 Side flow

The material flowing to the side on the edges of the grooves are indicators of plasticity where the material is allowed to deform freely under the loading of the indenter during the scratch. Specifically, the side flow may be seen as the exemplary egression of dislocations through the free surface during slip activation. Suppression of this material flow is observed under the mechanochemical effect of up to 56%, which is consistent with the elaboration on the mechanochemical influence on the material. Such suppression in plastic deformation was also observed in cutting chips produced during micro-cutting, which was believed to result in embrittlement [10] and dynamic recrystallization of the chips [11]. It is interesting to note, however, that the height of the side flow is rather consistent across the different surface areas. Such an observation is reasonable as the differences in the surfaces were along the scratch direction, while the lateral direction remained relatively constant across the different surfaces. Nonetheless, the presence of the SAM on the surface served its purpose of favorably bonding with the surface workpiece atoms to restrict dislocation egression through the surface. Hence, plasticity was restricted on the surface and the material flow was constricted resulting in lower side flow heights.

3.2.3 Elastic recovery

Another area of influence by the mechanochemical effect is on

the elastic recovery, which was assessed by comparing the penetration depth measured during the scratch process with the final measured depth. A higher magnitude of elastic recovery was observed without the SAM. For example, a comparison of the data shown in Figs. 5 and 6 shows that the penetration depth of up to 11.4 μm had an 89% recovery to a final residual depth of 1.2 μm for the surface without SAM. On the other hand, the chemisorbed surface exhibited an 81% recovery from 4.2 μm to 0.8 μm .

4. Conclusions

The effect of sample surface area exposed to chemisorption during application of the mechanochemical effects was investigated in this work through scratching tests with ink as a surface-active medium (SAM) on RSA6061. The penetration depth drastically reduced by up to 63.2% with SAM alongside lower residual depth. The mechanochemical effect progressively showed stronger manifestations with the increase in surface area. However, the relationship between surface area and the magnitude of the mechanochemical effect were non-linear suggesting potential effects of morphology of the surface deformities. Scratch hardness was increased by 18.2% under the mechanochemical effect. Moreover, there were limited deformation of the material in both the scratching depths and the material flow to the side of the grooves. Further investigation on the direct impact of surface area on the manifestation of the mechanochemical effect is necessary. At this juncture, the geometry of the surface deformities is likely a potential cause for non-linear relationship between surface area and mechanochemical effects.

ACKNOWLEDGEMENTS

The authors are grateful for the support from the Ministry of Education, Singapore, Grant nos.: MOE-T2EP50220-0010, MOE-T2EP50120-0010.

REFERENCES

1. Udupa, A., Viswanathan, K., Saei, M., Mann, J.B., and Chandrasekar, S., "Material-independent mechanochemical effect in the deformation of highly-strain-hardening metals," *Phys. Rev. Appl.*, Vol. 10, No. 1, pp. 014009, 2018.
2. Davis, J.M., Saei, M., Mohanty, D.P., Udupa, A., Sugihara, T. and Chandrasekar, S., "Cutting of tantalum: Why it is so difficult and what can be done about it," *Int. J. Mach. Tools Manuf.*, Vol. 157, pp. 103607, 2020.
3. Zhang, J., Lee, Y.J. and Wang, H., "Surface texture transformation in micro-cutting of AA6061-T6 with the Rehbinder effect," *Int. J. Precis. Eng. Manuf.-Green Tech.*, Vol. 8, pp. 1151–1162, 2020.
4. Zheng, Z., Lee, Y.J., Zhang, J., Jin, X. and Wang, H., "Ultra-precision micro-cutting of maraging steel 3J33C under the influence of surface-active medium," *J. Mater. Process. Technol.*, Vol. 292, pp. 117054, 2021.
5. Shchukin, E.D., Goryunov, Y.V., Pertsov, N.V. and Bryukhanova, L.S., "Development of investigations of the adsorption reduction of strength of solids in the works of P. A. Rehbinder and his school," *Sov. Mater. Sci. a Transl. Fiz. Mekhanika Mater. /Acad. Sci. Ukr. SSR.*, Vol. 14, pp. 341–346, 1978.
6. Rehbinder, P.A. and Shchukin, E.D., "Surface phenomena in solids during deformation and fracture processes," *Prog. Surf. Sci.*, Vol. 3, pp. 97–188, 1972.
7. Lee, Y.J. and Wang, H., "Current understanding of surface effects in microcutting," *Mater. Des.*, Vol. 192, pp. 108688, 2020.
8. Chaudhari, A., Soh, Z.Y., Wang, H. and Kumar, A.S., "Rehbinder effect in ultraprecision machining of ductile materials," *Int. J. Mach. Tools Manuf.*, Vol. 133, pp. 47–60, 2018.
9. Rahman, M.A., Amrun, M.R., Rahman, M. and Kumar, A.S., "Variation of surface generation mechanisms in ultra-precision machining due to relative tool sharpness (RTS) and material properties," *Int. J. Mach. Tools Manuf.*, Vol. 115, pp. 15–28, 2017.
10. Lee, Y.J., Shen, Y.K. and Wang, H., "Suppression of polycrystalline diamond tool wear with mechanochemical effects in micromachining of ferrous metal," *J. Manuf. Mater. Process.*, Vol. 4, No. 3, pp. 81, 2020.
11. Zhang, J., Lee, Y.J. and Wang, H., "Microstructure evaluation of shear bands of microcutting chips in AA6061 alloy under the mechanochemical effect," *J. Mater. Sci. Technol.*, Vol. 91, pp. 178–186, 2021.
12. Arcona, C., and Dow, T.A., "An empirical tool force model for precision machining," *J. Manuf. Sci. Eng.*, Vol. 120, pp. 700–707, 1998.